NJC

PAPER

Synthesis and 2D self-assembly at the liquid–solid interface of novel H-bonding linear π-conjugated oligomers terminated by uracil and melamine units†

G. Y. Y. Chng,[a] X. Sun,[bc] S. J. Cho,[a] D. Rajwar,[a] A. C. Grimsdale*[a] and D. Fichou*[bc]

Cite this: *New J. Chem.*, 2014, **38**, 2407

Received (in Montpellier, France) 18th December 2013, Accepted 25th February 2014

DOI: 10.1039/c3nj01606d

www.rsc.org/njc

We report here on the synthesis and 2D self-assembly of novel H-bonding linear π-conjugated oligomers terminated at both ends by either two uracil moieties (compound **GR1**) or by two melamine groups (compounds **GR2** and **GR3**). The bis(uracil) **GR1** compound was prepared by Sonogashira coupling of an ethynyluracil with a dihalobenzene and characterized spectroscopically. The synthesis of **GR2** and **GR3** was performed by Suzuki coupling of the dihalogenated benzene derivatives leading to the respective bisadducts which were then converted into the target bis-melamine derivatives by treatment with dicyanodimide. Self-assembly of the **GR1** derivative is investigated at the liquid/graphite interface using scanning tunneling microscopy (STM). When deposited from *n*-tetradecane, **GR1** forms a row-like structure stabilized by multiple terminal H-bonds between neighboring molecules. Co-adsorption of two *n*-tetradecane molecules per unit cell is also clearly identified. In turn, when deposited from 1-phenyloctane **GR1** forms a complex quasi square-shaped open structure having asymmetric sides. One possible arrangement is that four phenyloctane molecules are co-adsorbed in-between **GR1** rows similar to those formed from *n*-tetradecane, thus forming the two other sides of the square-shaped motif. From both solvents, the row-like 2D arrangements are governed by the multiple terminal H-bonds which create long-range alignments in one direction and by the van der Waals interdigitation of the dodecyl chains of the **GR1** molecules that stabilize the network in a nearly perpendicular direction.

Introduction

Small π-conjugated organic molecules have been widely developed as active materials in various electronic devices such as photovoltaic solar cells, field-effect transistors, light-emitting diodes, or sensors.[1–5] They can easily be processed as homogeneous thin films either from solution or by vacuum-deposition and then potentially lead to low-cost manufacturing, enable the use of flexible substrates and allow fabrication of large-area components. In contrast to polymers, small organic molecules are prone to form highly-ordered materials resulting in substantial improvements in the performances of organic-based devices. Two-dimensional (2D) self-assembly of appropriate molecular building blocks on surfaces is a widely-used strategy to prepare nanostructured functional architectures with pre-defined geometry and properties.[6–13] In particular, H-bonds have been extensively used to direct the 2D self-assembly taking advantage of the lower energy compared to covalent bonds as well as spatial directionality. Adsorption of trimesic acid

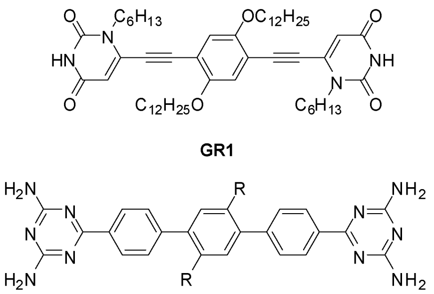

GR1

GR2 R = $OC_{12}H_{25}$, 58%
GR3 R= C_8H_{17} , 50%

Scheme 1 Chemical formulae of the three compounds under study here.

---

[a] School of Materials Science and Engineering, Nanyang Technological University, Singapore. E-mail: ACGrimsdale@ntu.edu.sg; Fax: +6567909081; Tel: +6567906728

[b] Sorbonne Universités, UPMC Univ Paris 06, UMR 8232, Institut Parisien de Chimie Moléculaire, F-75005, Paris, France. E-mail: denis.fichou@upmc.fr; Fax: +33144275572; Tel: +33144275080

[c] CNRS, UMR 8232, Institut Parisien de Chimie Moléculaire, F-75005, Paris, France

† Electronic supplementary information (ESI) available: Synthetic details of the preparation of the precursors of **GR1**, **GR2** and **GR3**; ^{1}H NMR spectra; MALDI TOF mass spectra; UV-visible absorption and photoluminescence spectra. See DOI: 10.1039/c3nj01606d

through OH′′′′O bonds on various surfaces constitutes the archetype of H-bond-driven self-assembled networks.[14,15] Various other types of H-bonding molecules such as N-containing molecules have also been reported for the formation of NH′′′′O or NH′′′′N H-bonded 2D nanostructures.[16–23] H-bonds can also allow different molecules to clip together to form two or three-component networks.[24,25] Finally, note that "weak" H-bonds, *e.g.* H-bonds with $E < 5$ kcal mol^{-1}, like for example CH′′′′O, have also been used to build self-assembled 2D arrays.[26]

We recently reported on the self-assembly of end-substituted star-shaped oligophenylenes.[27] In the present study, our aim is to elaborate extended 2D networks by linking together suitable functional molecules through non-covalent interactions such as H-bonds. These hollow site networks might plausibly be made by the non-covalent interaction of two units of trigonal and linear shape, respectively, and bearing complementary functional groups. Incorporation of appropriate guest organic molecules, metallic atoms or inorganic quantum dots into the nanocavities within these networks would result in multi-component materials with optoelectronic properties suitable for use in devices such as photovoltaic devices. These networks could be made by the non-covalent interaction of two units, one trigonal and the other linear, bearing complementary H-bonding groups.

Along with this approach, we now report the synthesis and 2D self-assembly of a linear molecule bearing a uracil moiety at each end (**GR1**) as well as the synthesis of two similar molecules terminated by melamine groups (**GR2** and **GR3**, Scheme 1). Uracil groups are capable of forming hydrogen bonds with melamine units. Thus co-deposition of such a molecule with a suitable melamine derivative might produce the desired extended networks.

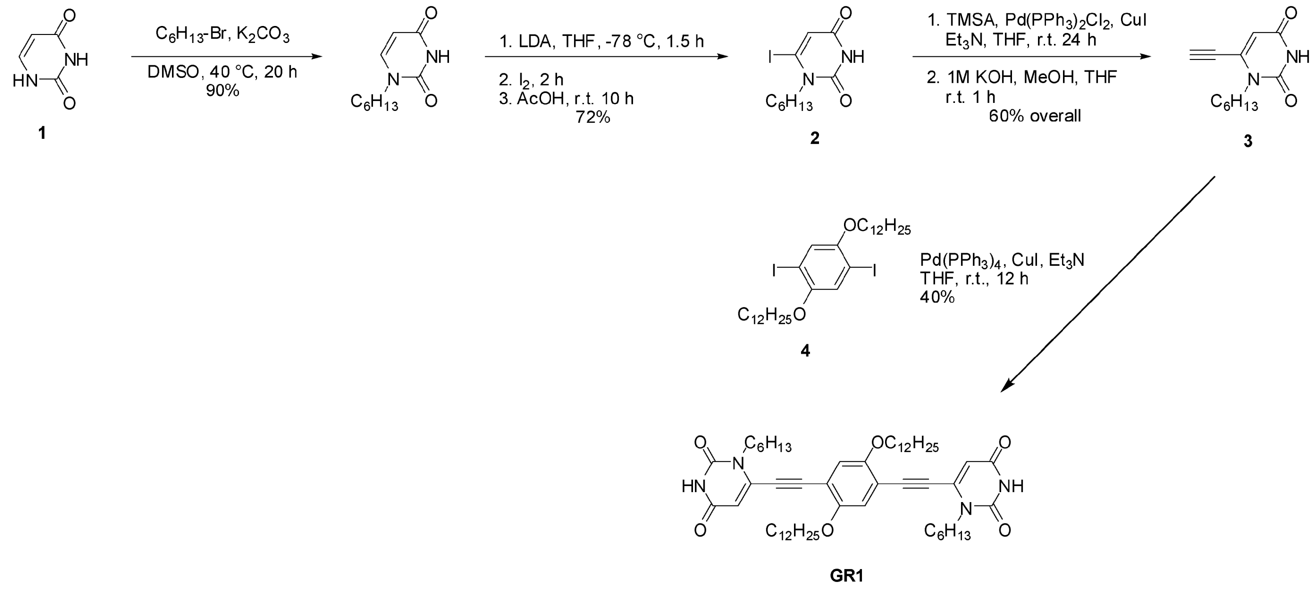

Scheme 2 Chemical pathway to the bis(uracil) compound **GR1**.

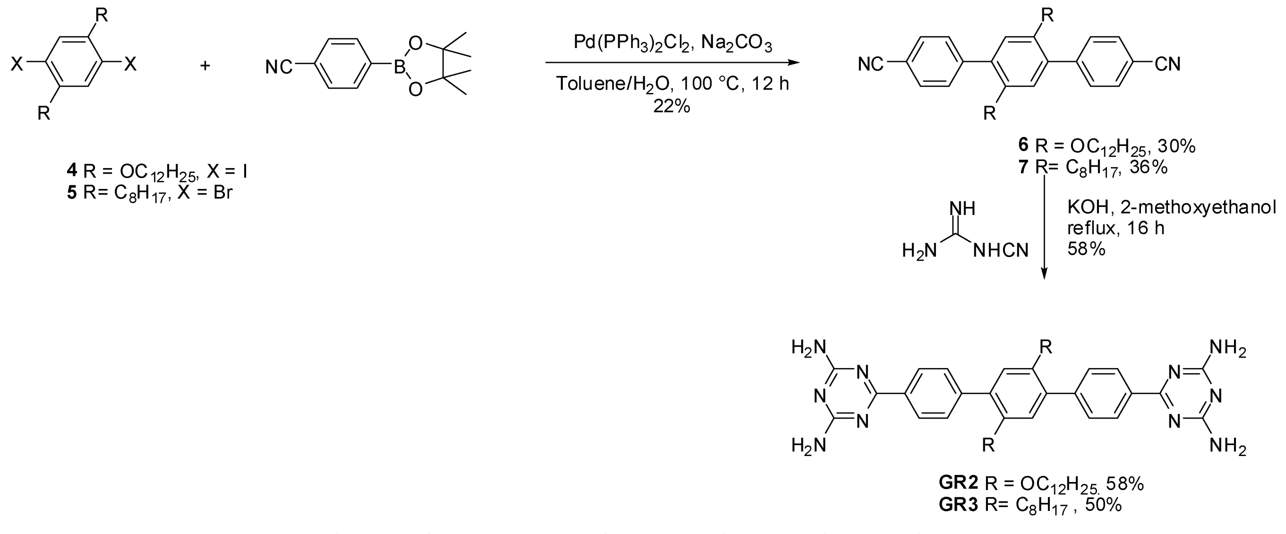

Scheme 3 Chemical pathway to the bis(melamine) compounds **GR2** (R = $OC_{12}H_{25}$) and **GR3** (R = C_8H_{17}).

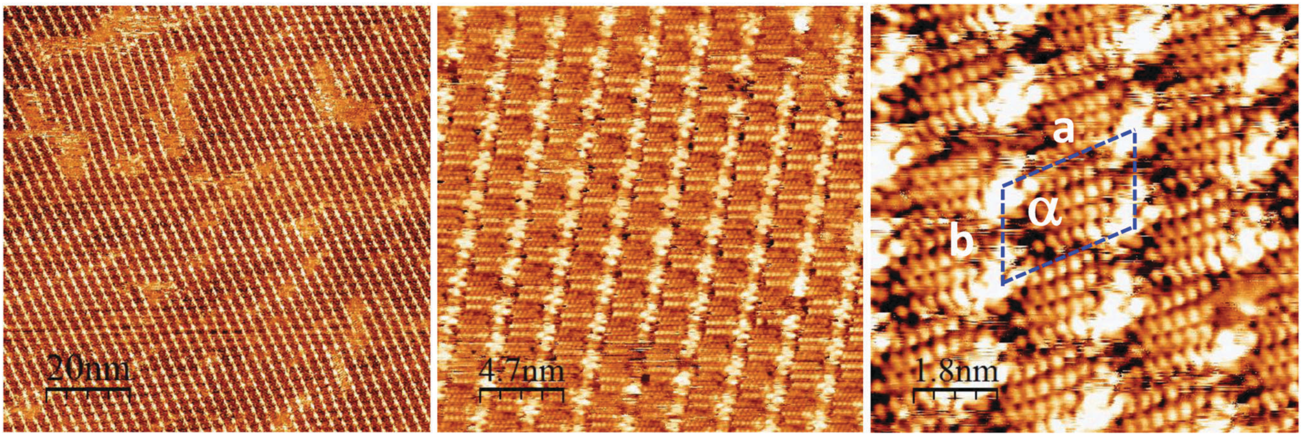

Fig. 1 STM images of the **GR1** self-assembly at the *n*-tetradecane/HOPG interface. Left: 100 × 100 nm^2, I_t = 20 pA, V_s = −0.6 V. Middle: 23.4 × 23.4 nm^2, I_t = 20 pA, V_s = −1.0 V. Right: 9 × 9 nm^2; I_t = 20 pA, V_s = −0.6 V. The unit cell is indicated by blue dashed lines.

This short oligomer has a relatively large bandgap and should be capable of transferring energy or electrons to a suitable co-monomer within the proposed networks or to a guest molecule deposited inside the network.

We reveal by means of scanning tunnelling microscopy (STM) that the 2D self-assembly of the linear derivative **GR1** forms long-range 2D networks when physisorbed at the HOPG/liquid interface. When deposited from *n*-tetradecane, **GR1** forms a row-like structure stabilized by multiple terminal H-bonds between neighbouring molecules. In turn, when 1-phenyloctane is used as the solvent we observe a square arrangement where molecules are interconnected through multiple H-bonds formed between neighbouring amino-diketo terminal groups. Attempts to produce two-component networks by combining **GR1** together with melamine or the **GR2** and **GR3** are currently in progress. Due to their limited solubility, the self-assembly of the melamine derivatives and of a mixture of the uracil and melamine-terminated molecules has not yet been investigated by STM.

Results and discussion

Synthesis of the GR1, GR2 and GR3 compounds

The bis(uracil) derivative **GR1** was prepared as shown in Scheme 2. Uracil **1** was first alkylated and then iodinated. The iodoalkyluracil **2** was then converted into the ethynyl derivative **3** by Sonogashira coupling with trimethylsilylacetylene followed by deprotection with a base. Sonogashira coupling with the diiododialkoxybenzene **4** then gave the desired molecule **GR1** as a yellow solid with 40% yield. The structure of **GR1** was confirmed by ^{1}H NMR, mass spectrometry, UV-visible absorption, fluorescence and IR spectroscopies (see ESI†). The **GR1** molecule shows an absorption maximum in chloroform at λ_{abs} = 375 nm and a photoluminescence maximum at λ_{em} = 450 nm (Fig. S6, ESI†).

Compounds **GR2** (R = $OC_{12}H_{25}$) and **GR3** (R = C_8H_{17}) bearing two terminal melamine moieties were synthesized as shown in Scheme 3. The Suzuki coupling[28] of the dihalides **4** and **5**[29,30] gave, respectively, the bisadducts **6** and **7**. These were then converted into the bis-melamine derivatives **GR2** and **GR3** by treatment with dicyanodimide.[31,32] The optical absorption and emission spectra of the dialokoxybenzene derivative **GR2** are similar to those of **GR1**, with two absorption maxima in the UV region (at 308 and 374 nm) and a single emission band peaking at ∼512 nm (Fig. S10, ESI†) By contrast, the dialkyl derivative **GR3** shows only one absorption band peaking at ∼295 nm and a blue-shifted emission band peaking at ∼430 nm (Fig. S15, ESI†).

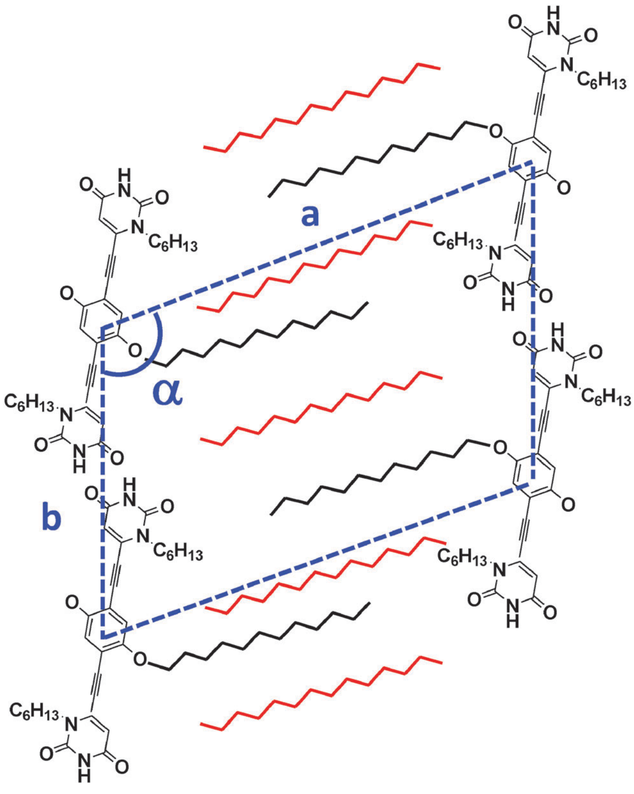

Fig. 2 Proposed model of the 2D structure of **GR1** at the *n*-tetradecane/HOPG interface. The unit cell is outlined by the blue dashed lines (*a* = 3.0 ± 0.1 nm; *b* = 2.0 ± 0.1 nm; *α* = 110 ± 1°). Co-adsorbed *n*-tetradecane molecules are indicated in red (two per unit cell). Hexyl chains of **GR1** are not represented because they are not visible on the STM images.

This is not surprising since alkoxy groups often induce a marked red-shift of the absorption and emission spectra as compared to similar compounds bearing alkyl groups. This well-known effect originates from the electron-donating nature of the alkoxy groups and has been extensively discussed.[33] Finally, note that the multiple hydrogen-bonding sites of the melamine groups make **GR2** and **GR3** poorly soluble in non-polar solvents.

Self-assembly of GR1 studied by STM at the liquid/HOPG interface

GR1 from *n*-tetradecane. When deposited from *n*-tetradecane on graphite the **GR1** molecules form large single domains whose size may extend well beyond 100 × 100 nm^2 (Fig. 1, left). The 2D self-organized monolayer network consists of alignments of **GR1** molecules into parallel rows. In the STM images the conjugated cores of **GR1** appear as parallel bright lines separated by a distance of ~3 nm. High-resolution reveals the details of the 2D arrangement (Fig. 1, right). Single **GR1** molecules are again well-resolved, with the lateral dodecyl chains clearly resolved as six bright spots. The hexyl chains of the **GR1** molecules are not directly observable probably because of their very short length. The unit cell is indicated by dashed blue lines in Fig. 1, right ($a = 3.0 \pm 0.1$ nm; $b = 2.1 \pm 0.1$ nm; $\alpha = 110 \pm 1°$). It contains one **GR1** molecule ($Z = 1$) and also two *n*-tetradecane molecules interdigitated with the dodecyl chains. A model of the arrangement is presented in Fig. 2. Importantly the **GR1** molecules are connected to each other in a head-to-head fashion through two H-bonds occurring between terminal NH and C=O groups (Scheme 4). Both the H-bonding between the neighboring **GR1** molecules and the van der Waals interaction between the neighboring alkyl chains play important roles in forming the **GR1** row-like supramolecular network on the HOPG surface.

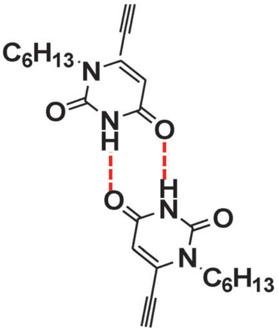

Scheme 4 Intermolecular terminal H-bonds (red dotted lines) stabilizing the **GR1** network.

GR1 from 1-phenyloctane. Long-range ordering appears immediately after deposition of **GR1** from 1-phenyloctane on HOPG. Highly ordered domains up to 50 × 50 nm^2 in size are observed, with the **GR1** molecules forming a quasi square-shaped structure (Fig. 3, left). Higher resolution (Fig. 3, middle and right) allows us to visualize the main cores of the molecules with the three interconnected rings. The two dodecyl chains are also clearly visible, appearing as six white spots inside the squares on the STM images. In between the two **GR1** molecules aligned vertically in the STM image of Fig. 3 appear four other bright spots having a contrast similar to that of the three individual aromatic rings of **GR1**. No alkyl chain is associated with these four bright spots but the distance separating the two molecules corresponds roughly to the length of a 1-phenyloctane molecule. Therefore we suggest that these spots correspond to the aromatic benzene cores of four co-adsorbed 1-phenyloctane molecules thus forming a bridge between consecutive **GR1** vertical rows.

Another possibility would be that the horizontal bridges between vertical rows are made of additional **GR1** molecules. However no additional dodecyl chains are observed, making such a hypothesis unlikely. The unit cell of the arrangement in 1-phenyloctane is represented by the blue lines in the STM image (Fig. 3) and in the proposed model (Fig. 4). The unit cell parameters are $a = b = 2.4 \pm 0.1$ nm, $\alpha = 92 \pm 1°$. In this model there is only one **GR1** molecule per unit cell ($Z = 1$) while there are four co-adsorbed 1-phenyloctane molecules, something rather unusual. The complexity of this arrangement is challenging and a more detailed analysis will be reported elsewhere.

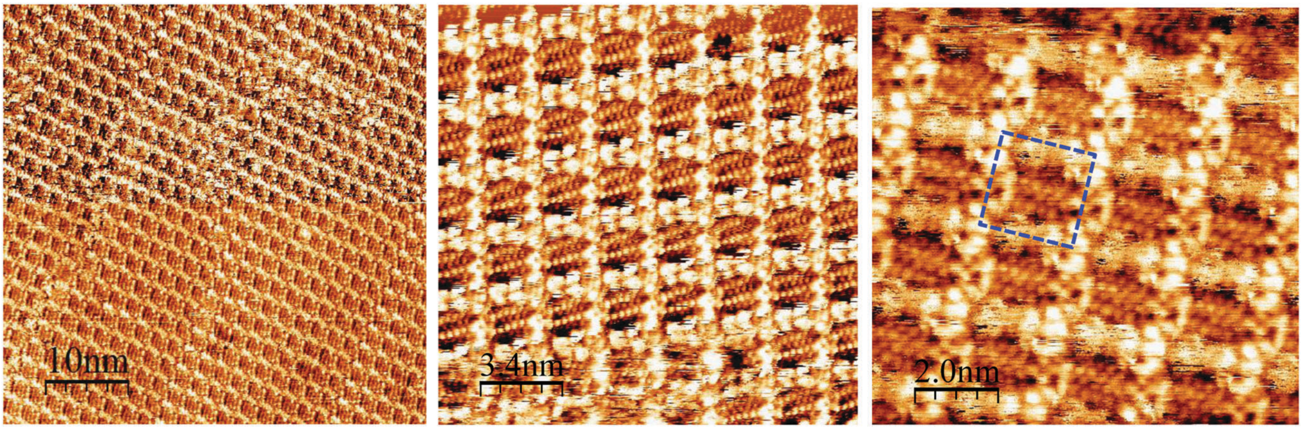

Fig. 3 STM images of **GR1** at the 1-phenyloctane/HOPG interface. Left: 50 × 50 nm^2; I_t = 10 pA, V_s = 0.8 V. Middle: 17 × 17 nm^2, I_t = 12 pA, V_s = 0.8 V. Right: 10 × 10 nm^2, I_t = 20 pA, V_s = 0.8 V. The quasi-square shaped unit cell is indicated as blue dashed lines.

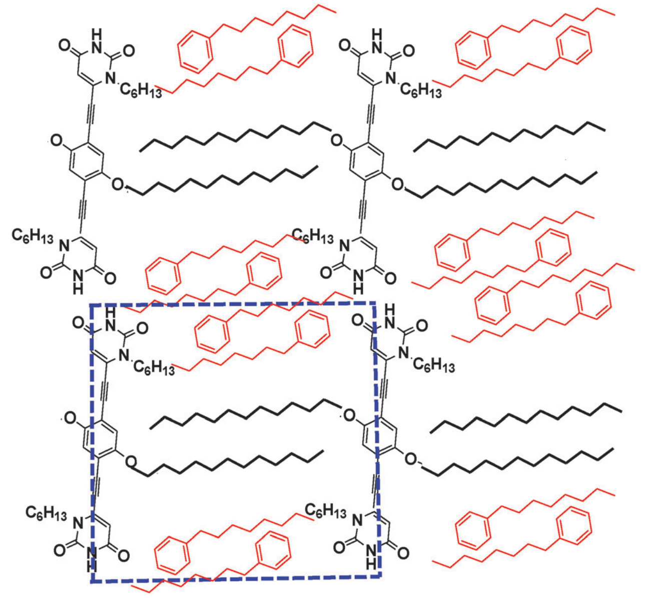

Fig. 4 Possible model of the **GR1** network with the co-adsorption of four 1-phenyloctane molecules per unit cell (in red on the scheme). The unit cell is indicated by blue dashed lines ($a = b = 2.4 \pm 0.1$ nm; $\alpha = 92 \pm 1°$).

Conclusion

In summary we have first described the synthesis of three novel linear π-conjugated oligomers terminated on both ends by H-bonding uracil and melamine units. The bis(uracil) **GR1** compound was prepared by Sonogashira coupling of an ethynyl-uracil with a dihalobenzene and characterized spectroscopically. Besides, the synthesis of **GR2** and **GR3** was performed by Suzuki coupling of the dihalogenated benzene derivatives leading to the respective bisadducts which were then converted into the target bis-melamine derivatives by treatment with dicyanodimide.

Then, by means of STM at the liquid/graphite interface, we have revealed that when deposited from *n*-tetradecane **GR1** forms a row-like structure stabilized by multiple terminal H-bonds between neighbouring molecules. Co-adsorption of two *n*-tetradecane molecules per unit cell is also clearly identified. In turn, when deposited from 1-phenyloctane **GR1** forms a complex quasi square-shaped open structure having asymmetric sides. One possible arrangement is that four 1-phenyloctane molecules are co-adsorbed in-between the **GR1** rows, thus forming the two other sides of the square-shaped motif. From both solvents, the row-like 2D arrangements are governed (1) by the multiple terminal H-bonds which create long-range alignments in one direction and (2) by the van der Waals interdigitation of the dodecyl chains of **GR1** that stabilize the network in the nearly perpendicular direction.

Finally, as stated in our introduction, we are presently investigating the possibility to clip the uracil **GR1** together with either of the melamine **GR2** or **GR3** by means of three complementary terminal H-bonds to form hybrid linear rows with an alternation of two different **GR** molecules. We are also mixing the **GR** molecules with trigonal star-shaped planar molecules bearing complementary H-bonding motifs synthetized in our lab[27] in order to produce 2D open networks with size-selected cavities.

Experimental section

Synthetic procedures

General methods. The starting compounds **1–5** (see Schemes 2 and 3) were prepared following literature procedures.[22,34,35] All other reagents and solvents were obtained commercially and used without further purification. NMR spectra were recorded on a Bruker Advance 400 MHz spectrometer. Mass spectra were obtained using a Shimadzu Axima MALDI-TOF mass spectrometer. UV-Visible absorption spectra were recorded on a Shimadzu UV-2501PC spectrophotometer. Photoluminescence spectra were measured on a Shimadzu RF-5301PC spectrofluorometer.

1,1′-Hexyl-6,6′-[(1,4-bis(dodecyloxy)-2,5-phenylene)diethynyl]-bisuracil (GR1). To a degassed solution of dry triethylamine (20 mL) and THF (20 mL), 1,4-bis(dodecyloxy)-2,5-diiodobenzene (0.77 g, 1.102 mmol), palladium catalyst (0.06 g, 0.052 mmol), and copper iodide (0.018 g, 0.095 mmol) were added and the mixture was degassed a second time. Ethynyl uracil derivative **3** (0.6 g, 2.72 mmol) was then added, and the reaction mixture was degassed one last time and stirred overnight at 85 °C under nitrogen. The mixture was filtered through Celite, and then the solvent was concentrated under vacuum. The precipitate was purified by several precipitations from chloroform upon addition of methanol, yielding GR1 (0.97 g, 40.3%) as a yellow solid. ^{1}H NMR (400 MHz, $CDCl_3$) δ 8.36 (br. s, 2H, NH), 6.97 (s, 2H), 4.10 (t, 4H), 4.01 (t, 4H) 1.78 (m, 8H), 1.44 (m, 4H), 1.30 (m, 44H), 0.86 (m, 12H). MALDI-TOF MS: m/z = 883.1 [M+] (calculated for $C_{54}H_{82}N_4O_6$ = 882.62). UV-Vis ($CHCl_3$) λ_{max} = 306, 320, 399 nm.

2,5-Bis(4′-cyanophenyl)-1,4-didodecyloxybenzene 6. 2,5-Diiodo-1,4-didodecyloxybenzene **4** (1.0 g, 1.43 mmol), 4-cyanophenyl-boronic ester (0.72 g, 3.15 mmol), 30 mL of THF–water (2 : 1), and sodium carbonate (10 mL, 20 mmol) were mixed in a 100 mL flask and degassed with nitrogen. After 10 minutes the palladium catalyst (0.221 g, 0.315 mmol) was added, and the mixture refluxed for 24 hours. The mixture was cooled to room temperature, and the organic phase was separated and filtered through Celite. The precipitate was purified by several precipitations from chloroform by addition of ethanol, yielding compound **6** as a white solid (0.28 g, 30%). ^{1}H NMR (400 MHz, DMSO-d_6) δ (ppm): 8.30 (d, J = 8 Hz, 4H), 7.65 (d, J = 8 Hz, 4H), 7.05 (s, 2H), 3.95 (t, 4H), 1.62–1.64 (br. m, 36H), 1.19–1.33 (br. m, 4H), 0.82 (t, 6H). ^{13}C NMR (100 MHz, DMSO-d_6) δ (ppm): 166.9, 149.7, 140.5, 129.6, 128.8, 127.2, 115.4, 68.7, 39.5, 31.2, 29.0, 28.9, 28.9, 28.6, 28.5, 25.4, 22.0, 13.8.

Melamine derivative GR2. To a mixture of compound **6** (300 mg, 0.46 mmol), powdered potassium hydroxide (0.143 g, 2.54 mmol) and dicyanodiamide (0.1 g, 2.57 mmol) 20 mL of 2-methoxyethanolwere added. The reaction mixture was stirred at 125 °C overnight, and then poured into dichloromethane. The organic layer was washed with water. Ethanol was added to the crude product to afford **GR2** as a white solid (0.22 g, 58%). ^{1}H NMR (400 MHz, DMSO-d_6) δ (ppm): 8.30 (d, J = 8 Hz, 8H, NH_2), 7.65

(d, J = 8 Hz, 8H), 7.05 (br. s, 4H), 6.70 (br. s, 12H), 3.97–3.94 (br. m, 8H), 1.63 (br. d, J = 8 Hz, 8H), 1.33–1.19 (br. m, 18H), 0.82 (t, 12H). ^{13}C NMR (100 MHz, DMSO-d$_6$) δ (ppm): 166.86, 149.74, 140.51, 129.58, 128.77, 127.22, 115.40, 68.71, 39.50, 31.21, 28.96, 28.93, 28.89, 28.64, 28.53, 25.40, 22.02, 13.79.

The two dodecyl groups of **GR2** are identified in the chemical shift range 0.80–1.64 ppm (46 protons) while the other protons are identified in the range 3.94–3.97 ppm (4 protons). The aromatic protons are observed at 6.70 ppm and 7.05 ppm corresponding to 10 protons. The chemical shifts in the ^{13}C NMR observed at 166.9, 149.7, 140.5, 129.6, 128.8, 127.2 and 115.4 ppm correspond to aromatic carbons. The carbon atoms of the alkoxy groups are identified by chemical shifts at 68.7, 31.2, 29.0, 28.9, 28.6, 28.5, 25.4, 22.0, 13.8 ppm.

2,5-Bis(4′-cyanophenyl)-1,4-dioctylbenzene 7. 2,5-Dibromo-1,4-dioctylbenzene 5 (1.0 g, 2.172 mmol), 4-cyanophenylboronic ester (1.045 g, 4.56 mmol), 30 mL of DME–water (2 : 1), and sodium carbonate (2.12 g, 20 mmol) were mixed in a 100 mL flask and degassed with nitrogen. After 10 minutes the palladium catalyst (0.152 g, 0.217 mmol) was added and the mixture refluxed for 24 hours. The mixture was cooled to room temperature, and the organic phase was separated and filtered through Celite. The organic filtrate was concentrated and ethanol was added to crystallize **7** as a white solid (0.39 g, 36%). ^{1}H NMR (400 MHz, CDCl$_3$) δ (ppm): 7.71 (d, 4H, J = 8 Hz), 7.44 (d, 4H, J = 8 Hz), 7.07 (s, 2H), 2.52–2.48 (br. m, 4H), 1.43–1.14 (br. m, 24H), 0.85–0.82 (br. m, 6H). ^{13}C NMR (100 MHz, CDCl$_3$) δ (ppm): 146.47, 139.85, 137.63, 131.95, 130.70, 130.01, 118.88, 110.87, 77.32, 77.00, 77.00, 76.68, 32.48, 31.76, 31.33, 29.38, 29.16, 29.07, 22.60, 14.07.

Melamine derivative GR3. To a mixture of compound 7 (300 mg, 0.594 mmol), powdered potassium hydroxide (0.183 g, 3.27 mmol) and dicyanodiamide (0.1 g, 1.189 mmol) 20 mL of 2-methoxyethanolwere added. The reaction mixture was stirred at 125 °C overnight, and then poured into dichloromethane. The organic layer was washed with water. Ethanol was added to the crude product to give **GR3** as a white solid (0.190 g, 50%). ^{1}H NMR (400 MHz, DMSO-d$_6$) δ (ppm): 8.32 (d, 4H, J = 8 Hz), 7.41 (d, 4H, J = 8 Hz), 7.12 (s, 2H), 6.72 (br. s, 8H), 2.57 (br. t, 4H), 1.39 (br. d, 4H, J = 8 Hz), 1.25–1.10 (br. m, 20H), 0.78 (t, 6H). ^{13}C NMR (100 MHz, DMSO-d$_6$) δ (ppm): 139.66, 138.37, 136.81, 130.15, 128.68, 127.53, 106.43, 39.50, 31.10, 30.74, 28.77, 28.52, 28.42, 26.68, 21.92, 13.56.

In the ^{1}H NMR spectrum, the two octyl groups of **GR3** are identified in the chemical shift range 0.76–1.40 ppm (30 protons) and 2.50–2.59 ppm (4 protons). The ten aromatic protons are observed at 6.72 (8 protons) and 7.12 ppm (2 protons). In the ^{13}C NMR spectrum, the chemical shifts observed at 139.7, 138.4, 136.8, 130.2, 128.7, 127.5 and 106.43 ppm correspond to the aromatic carbon atoms.

Scanning tunnelling microscopy

Scanning tunnelling microscopy (STM) was performed using a PicoSPM (Molecular Imaging/Agilent Technology) equipped with a home-built liquid cell. The microscope was isolated from vibrations and noise inside a closed box with mechanical suspensions. The STM tips were mechanically cut from a platinum–iridium wire (Pt–Ir 90/10, diameter 0.25 mm, Goodfellow). The **GR1** molecules were dissolved in either *n*-tetradecane (99 + % purity, Aldrich) or 1-phenyloctane (98 + % purity, Aldrich) as the transfer solvents and tunnelling media. The saturated solutions were systematically diluted twice prior to deposition on the substrate. Samples of highly pyrolytic graphite (HOPG, 1 × 1 cm^2, Goodfellow) were freshly prepared by cleavage using adhesive tape prior to deposition, producing clean atomically flat surfaces. STM images were recorded at the liquid/HOPG interface in the constant-current mode (I_t). Applied biases were referred to the sample and V_s was noted throughout this study. The distance and angle values measured from the STM images are systematically averaged from two consecutive scans. All STM measurements were carried out at room temperature. STM images were processed and analyzed using the software WSXM 5.0.[36]

Acknowledgements

DF wishes to thank the Nanyang Technological University (NTU) for a Visiting Professor position in the School of Physical and Mathematical Sciences (SPMS), Division of Physics and Applied Physics (PAP). Funding through the Singapore Ministry of Education, Academic Research Fund Tier 1 (grant RG19/07) including a research student scholarship for DR, and funding through the National Research Foundation CRP Grant 5-2009-04 "Towards Efficient Sunlight Harvesting", are gratefully acknowledged.

Notes and references

1 Y. Sun, G. C. Welch, W. L. Leong, C. J. Takacs, G. C. Bazan and A. J. Heeger, *Nat. Mater.*, 2012, **11**, 44–48.

2 A. C. Grimsdale and K. Müllen, *Angew. Chem., Int. Ed.*, 2005, **44**, 5592–5629.

3 D. Fichou, *J. Mater. Chem.*, 2000, **10**, 571–588.

4 G. Xing, N. Mathews, S. Sun, S. S. Lim, Y. M. Lam, M. Grätzel, S. G. Mhaisalkar and T. C. Sum, *Science*, 2013, **342**, 344–347.

5 J. Zhou, Y. Zuo, X. Wan, G. Long, Q. Zhang, W. Ni, Y. Liu, Z. Li, G. He, C. Li, B. Kan, M. Li and Y. Chen, *J. Am. Chem. Soc.*, 2013, **135**, 8484–8487.

6 J. V. Barth, G. Costantini and K. Kern, *Nature*, 2005, **437**, 671–679.

7 R. Otero, F. Rosei and F. Besenbacher, *Annu. Rev. Phys. Chem.*, 2006, **57**, 497–525.

8 S. Furukawa and S. De Feyter, *Top. Curr. Chem.*, 2009, **287**, 87–133.

9 L. Piot, J. Wu, A. Marchenko, K. Müllen and D. Fichou, *J. Am. Chem. Soc.*, 2005, **127**, 16245–16250.

10 H. L. Zhang, W. Chen, H. Huang, L. Chen and A. T. S. Wee, *J. Am. Chem. Soc.*, 2008, **130**, 2720–2721.

11 A. Nion, P. Jiang, A. Popoff and D. Fichou, *J. Am. Chem. Soc.*, 2007, **129**, 2450–2451.

12 A. Stannard, J. C. Russell, M. O. Blunt, C. Salesiotis, M. del Carmen Gimenez-Lopez, N. Taleb, M. Schroder, N. R. Champness, J. P. Garrahan and P. H. Beton, *Nat. Chem.*, 2012, **4**, 112–117.

13 L. Piot, F. Silly, L. Tortech, Y. Nicolas, P. Blanchard, J. Roncali and D. Fichou, *J. Am. Chem. Soc.*, 2009, **131**, 12864–12865.

14 M. Lackinger, S. Griessl, W. M. Heckl, M. Hietschold and G. W. Flynn, *Langmuir*, 2005, **21**, 4984–4988.

15 O. Ivasenko and D. F. Perepichka, *Chem. Soc. Rev.*, 2011, **40**, 191–206.

16 S. Griessl, M. Lackinger, M. Edelwirth, M. Hietschold and W. M. Heckl, *Single Mol. Biol.*, 2002, **3**, 25–31.

17 A. Popoff and D. Fichou, *Colloids Surf., B*, 2008, **63**, 153–158.

18 A. L. Kanibolotsky, I. F. Perepichka and P. J. Skabara, *Chem. Soc. Rev.*, 2010, **39**, 2695–2728.

19 N. Katsonis, A. Marchenko and D. Fichou, *J. Am. Chem. Soc.*, 2003, **125**, 13682–13683.

20 J. M. MacLeod, O. Ivasenko, C. Fu, T. Taerum, F. Rosei and D. F. Perepichka, *J. Am. Chem. Soc.*, 2009, **131**, 16844–16850.

21 N. Saettel, N. Katsonis, A. Marchenko, M.-P. Teulade-Fichou and D. Fichou, *J. Mater. Chem.*, 2005, **15**, 3175–3180.

22 A. Llanes-Pallas, C.-A. Palma, L. Piot, A. Belbakra, A. Listorti, M. Prato, P. Samori, N. Armaroli and D. Bonifazi, *J. Am. Chem. Soc.*, 2009, **131**, 509–520.

23 I. Bestel, N. Campins, A. Marchenko, D. Fichou, M. W. Grinstaff and P. Barthélémy, *J. Colloid Interface Sci.*, 2008, **323**, 435–440.

24 R. Madueno, M. T. Räisänen, C. Silien and M. Buck, *Nature*, 2008, **454**, 618–621.

25 F. J. M. Hoeben, J. Zhang, C. C. Lee, M. J. Pouderoijen, M. Wolffs, F. Würthner, A. P. J. Schenning, E. W. Meijer and S. De Feyter, *Chem.–Eur. J.*, 2008, **14**, 8579–8589.

26 A. Popoff and D. Fichou, *J. Mol. Struct.*, 2009, **936**, 156–161.

27 D. Rajwar, X. Sun, S. J. Cho, A. C. Grimsdale and D. Fichou, *CrystEngComm*, 2012, **14**, 5182–5187.

28 B. Liu, T. T. T. Dan and G. C. Bazan, *Adv. Funct. Mater.*, 2007, **17**, 2432–2438.

29 A. Hilberer, H.-J Brouwer, B.-J. Van der Scheer, J. Wildeman and G. Hadziioannou, *Macromolecules*, 1995, **28**, 4525–4529.

30 K. T. Nielsen, H. Spanggaard and F. C. Krebs, *Macromolecules*, 2005, **38**, 1180–1189.

31 W.-L. Tong, M. C. W. Chan, N. Zhu and S.-K. Leung, *Dalton Trans.*, 2009, 4741–4746.

32 P. G. A. Janssen, J. L. J. van Dongen, E. W. Meijer and A. P. H. J. Schenning, *Chem.–Eur. J.*, 2009, **15**, 352–360.

33 A. C. Grimsdale, K. L. Chan, R. E. Martin, P. G. Jokisz and A. B. Holmes, *Chem. Rev.*, 2009, **109**, 897–1091.

34 L. Piot, C.-A. Palma, A. Llanes-Pallas, M. Prato, Z. Szekrenyes, K. Kamaras, D. Bonifazi and P. Samori, *Adv. Funct. Mater.*, 2009, **19**, 1207–1214.

35 C. Xue and F.-T. Luo, *Tetrahedron*, 2004, **60**, 6285–6294.

36 I. Horcas, R. Fernandez, J. M. Gomez-Rodriguez, J. Colchero, J. Gomez-Herrero and A. M. Baro, *Rev. Sci. Instrum.*, 2007, **78**, 013705.